CSIRO PUBLISHING
www.publish.csiro.au/journals/eg
Exploration Geophysics, 2007, **38**, 89–97

Three-dimensional magnetotelluric surveys for geothermal development in Pohang, Korea

Tae Jong Lee[1,3] Yoonho Song[1] Toshihiro Uchida[2]

[1]Korea Institute of Geoscience and Mineral Resources (KIGAM), Gajeong-dong 30, Yuseong-gu, Daejeon 305-350, Korea.
[2]Institute for Geo-resources and Environment (GREEN), AIST, Japan.
[3]Corresponding author. Email: megi@kigam.re.kr

Abstract. A three-dimensional (3D) magnetotelluric (MT) survey has been carried out to delineate subsurface structures and possible fractures, for development of low-temperature geothermal resources in Pohang, Korea. Quite good quality MT data could be obtained throughout the survey region by locating the remote reference in Kyushu, Japan, which is ~480 km from the centre of the field site.

3D modelling and inversion are performed taking into account the sea effect in MT measurements near the seashore. The nearby sea in the Pohang area affects MT data at frequencies below 1 Hz ~0.2 Hz, depending on the distance from the seashore. The most severe sea effects were observed in the south-east parts of the survey area, closer to Youngil Bay. 3D inversion with and without the seawater constraint showed very similar results at shallow depths, roughly down to 2 km. At greater depths, however, a strong sea effect seems to form a fictitious conductive structure in ordinary 3D inversion, especially in the south-eastern part of the survey region.

Comparison between drilling results and the resistivity profiles from inversions showed that five layered structures can be distinguished the subsurface beneath the target area. They are: (a) semi-consolidated mudstones with resistivity less than 10 Ω m, which are ~300 m thick in the northern part and ~600 m thick in the southern part of the survey area; (b) occasional occurrence of trachybasalt and lapilli tuff within the mudstone layer has resistivity of a few tens of Ω m, (c) intrusive rhyolite ~400 m thick has resistivity of several hundreds of Ω m, (d) alternating sandstone and mudstone down to 1.5 km depth shows resistivity of ~100 Ω m, (e) a conductive structure was found at a depth of ~3 km, but more geological and geophysical study should be carried out to identify this structure.

Key words: 3D MT survey, geothermal exploration, remote reference MT, sea effect.

Introduction

In 2002 and 2003, dense three-dimensional (3D) magnetotelluric (MT) surveys were carried out for geothermal exploration in Pohang, Korea, in a joint research program of the Korea Institute of Geoscience and Mineral Resources (KIGAM) and the Institute for Geo-Resources and Environment, Geological Survey of Japan (AIST).

Korea is one of the most difficult countries in the world for MT data acquisition because artificial electromagnetic noise from power lines and various other man-made sources is extremely strong over almost the whole country. What is worse is that the country is mostly underlain by relatively old formations that generally have high resistivity, through which electromagnetic (EM) noise can propagate to great distances. We therefore used a very distant remote reference by setting up a remote site in south-western Japan in order to overcome the noise. The approximate distance between the survey area and the remote station is ~480 km. As well as the remote reference in Japan, we also installed a remote reference site within the Korean peninsula for comparison purposes.

Pohang is located on the south-east margin of the Korean peninsula, and the survey area lies very close to the sea shore. The boundary between the sea and land induces severe distortion of electrical fields because of its extremely high conductivity contrast. There have been several efforts to identify and to correct ocean or coast effects in MT and geomagnetic depth sounding (GDS) data (Monteiro Santos et al., 1999, 2006; Bapat et al., 1993; Oh et al., 2003). MT measurements on the Korean peninsula, surrounded by seas on three sides, will not be free from the sea effect. Of the seas surrounding Korea, the East Sea is the deepest, ten times deeper than the West Sea and the South Sea of Korea, and thus has the most severe effects on low-frequency EM measurements on the eastern side of Korean peninsula, including the Pohang area (Oh et al., 2003). Bapat et al. (1993) have performed an induction arrow analysis by numerical thin sheet modelling, and showed that the overall pattern of induction arrows at low frequencies on the eastern side of the Korean peninsula points toward the East Sea at low frequencies, because of the sea effect.

In this study, we first perform 3D modelling for a sea model to infer the sea effect in the observed MT data from our Pohang site. The 3D model is set up to include simplified coastline nearby, layering of subsurface structure, and average resistivity of each layer down to 1.5 km, based on results from test drilling, and assumes average depth for the bathymetry of the East Sea and average conductivity of the sea water. We then perform a 3D inversion with such geological settings as constraints and compare the results with the ordinary 3D inversion results.

Geology and lineaments

The survey area is located north of Pohang City, south-eastern Korea. Figure 1 shows the general geology and a lineament

10.1071/EG07004 0812-3985/07/010089

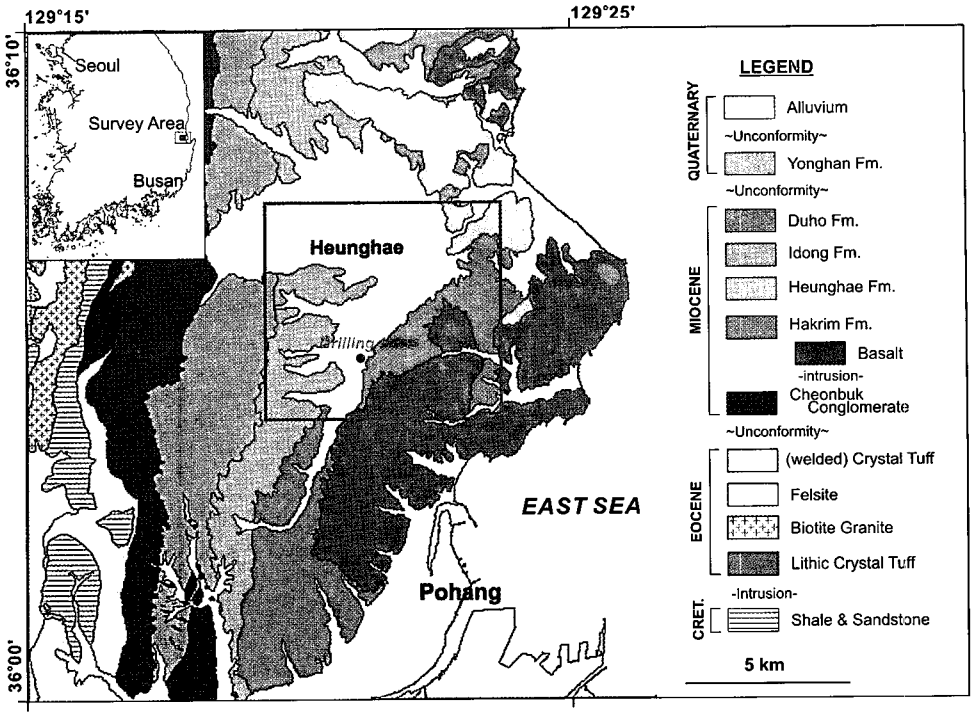

Fig. 1. (a) Geological map and (b) lineament distribution around the survey site (Song, 2004). The green box indicates the survey area.

distribution from a Landsat image of the survey area. The area lies in the Tertiary Pohang Basin, overlying Cretaceous sedimentary rocks with biotite-granite, rhyolite, and trachybasalt intrusions (Song, 2004). The Pohang Basin consists of Miocene marine sediments and a clastic sediment layer at the base. The Heunghae Basin, the main target for geothermal exploration, is covered with Quaternary alluvium underlain by thick Tertiary sediments, which are characterised by a semi-consolidated and highly conductive mudstone ($< 10\ \Omega$ m). This Tertiary sediment formation has relatively low thermal conductivity and thus preserves a high geothermal gradient, which is quite uncommon in Korea. A MT survey has been carried out over this Quaternary Heunghae Basin, enclosed by rectangles in Figure 1. Lineaments from the Landsat image are mainly NNE-SSW in the region, and two major lineaments, in the NNE-SSW and WNW-ESE directions, intersect within the MT survey region (Figure 1b).

Remote reference MT data acquisition and analysis

MT surveys have been conducted in two years, 2002 and 2003, and Figure 2 shows the survey map. A total of 70 measurements were made during this time. The 3D interpretation in this study is based on the data from the 44 sites within the rectangle in Figure 2. Two test boreholes, 165 m apart, were drilled in the year 2003–2004, one of them to a depth of 1.5 km. Various well logs including caliper, gamma ray, and resistivity have been acquired, so that the layered structures, resistivity of each layer, and fractures intersecting the boreholes can be investigated. The location of the test boreholes is also shown in Figure 2.

Measurements at each site were made during two nights for 15 h each, from 17:00 to 08:00 next day in local time, using a MTU-5A system by Phoenix Geophysics. The MTU-5A system is designed for tensor measurements, including two electric and three magnetic components at the surface, with 24-bit resolution for both AMT and MT bands. GPS synchronisation allows us to place a remote reference site as far as a few hundred kilometres, so that the electromagnetic noise is unlikely to be coherent with the field station signal. Remote reference processing was done with SSMT2000 software, developed by Phoenix Geophysics, Ltd.

Because Korea suffers extremely strong EM noise, as discussed in the Introduction, a remote reference was installed in Kyushu, Japan (RR_J in Figure 2, ~480 km from the survey area), where it appears to be relatively quiet in an EM noise sense. For the purpose of comparison, we also set up two remote reference sites in Korea; Andong in 2002 (RR1 in Figure 2) and Chungwon in 2003 (RR2 in Figure 2), which are ~60 km and 165 km from the centre of the survey area, respectively.

Figure 3 compares MT impedances (apparent resistivities and phases) at site PHG-415, which is close to the test boreholes, after remote reference processing with RR2 and RR_J. In the single-site impedance curves (Figure 3a), observe that the estimated impedances are severely contaminated by near-field noise, especially in the frequency range from 0.1 to 10 Hz. The phase goes almost to 0° (or −180°) in both *xy* and *yx* modes, and the apparent resistivity curve, especially in the *xy* components, has a steep gradient of ~45°. Here, the term '*xy* mode' refers to impedance estimation using E_x and H_y fields, where *x* points to the north.

Most of this near-field noise was removed by remote reference processing with RR2, as can be seen in Figure 3b. One can, however, still find some noise remaining at frequencies around 0.1 Hz, the so-called dead band, where the MT signal is weak. Ambient background noise seems commonly to affect both the field site and the remote site in Korea. When processed with data from the remote reference site in Japan (RR_J), this portion is much improved (Figure 3c), and resulting apparent resistivity and phase curves are seen to be quite continuous with respect to frequency. Comparing the outcome of processing with each of the three remote reference data sources, RR_J generally gave the best quality results.

Finally, starting with impedance values calculated automatically using RR_J, the MT impedances were manually edited by removing outlier segments, or large-variance segments, taking into consideration the Tipper magnitude and coherency as well as the continuity of the apparent resistivity and phase curves at neighbouring frequencies. If strong noise exists only within specific time segments within the 30 h of recording, we can improve the final data quality by eliminating those bad segments.

Figure 4 shows the induction arrows for all 70 sites, at frequencies 8 Hz, 0.3 Hz, and 0.01 Hz, derived from the observed magnetic fields. They are drawn with a sign convention so that

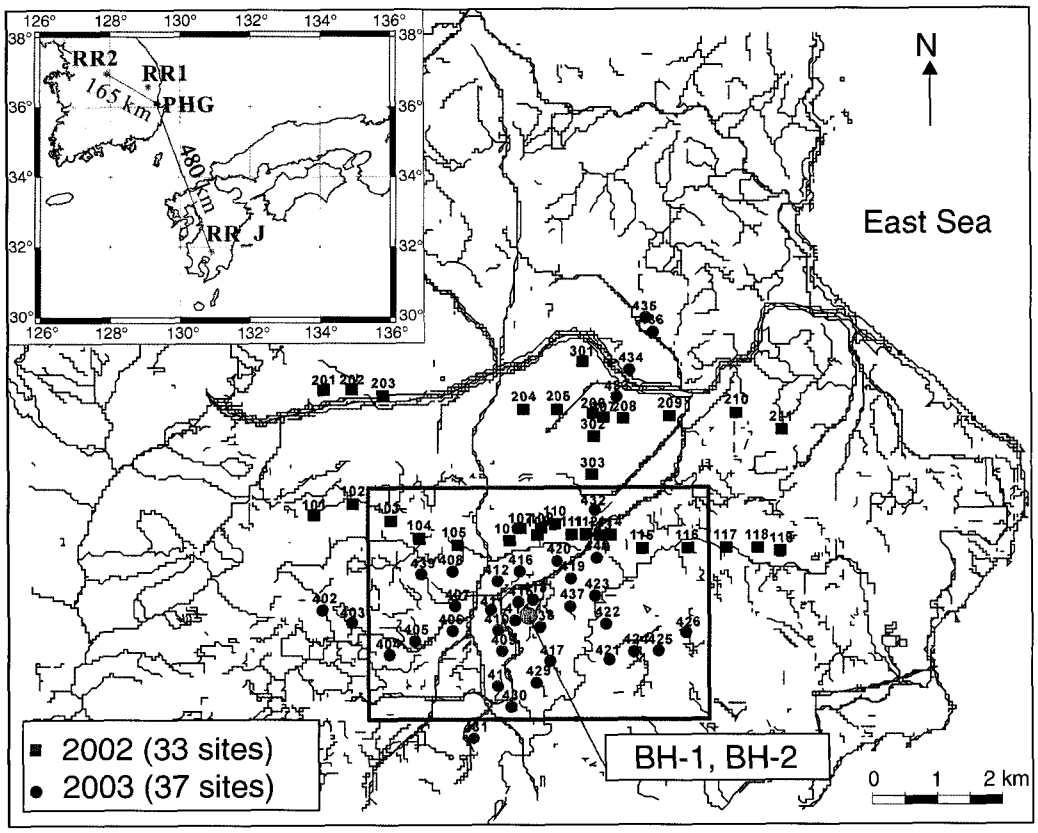

Fig. 2. Sitemap of the 3D MT survey, with the location of two remote reference sites in Korea (RR1,'RR2) and a remote reference site in Kyushu, Japan. The rectangle surrounds the region used for 3D interpretation.

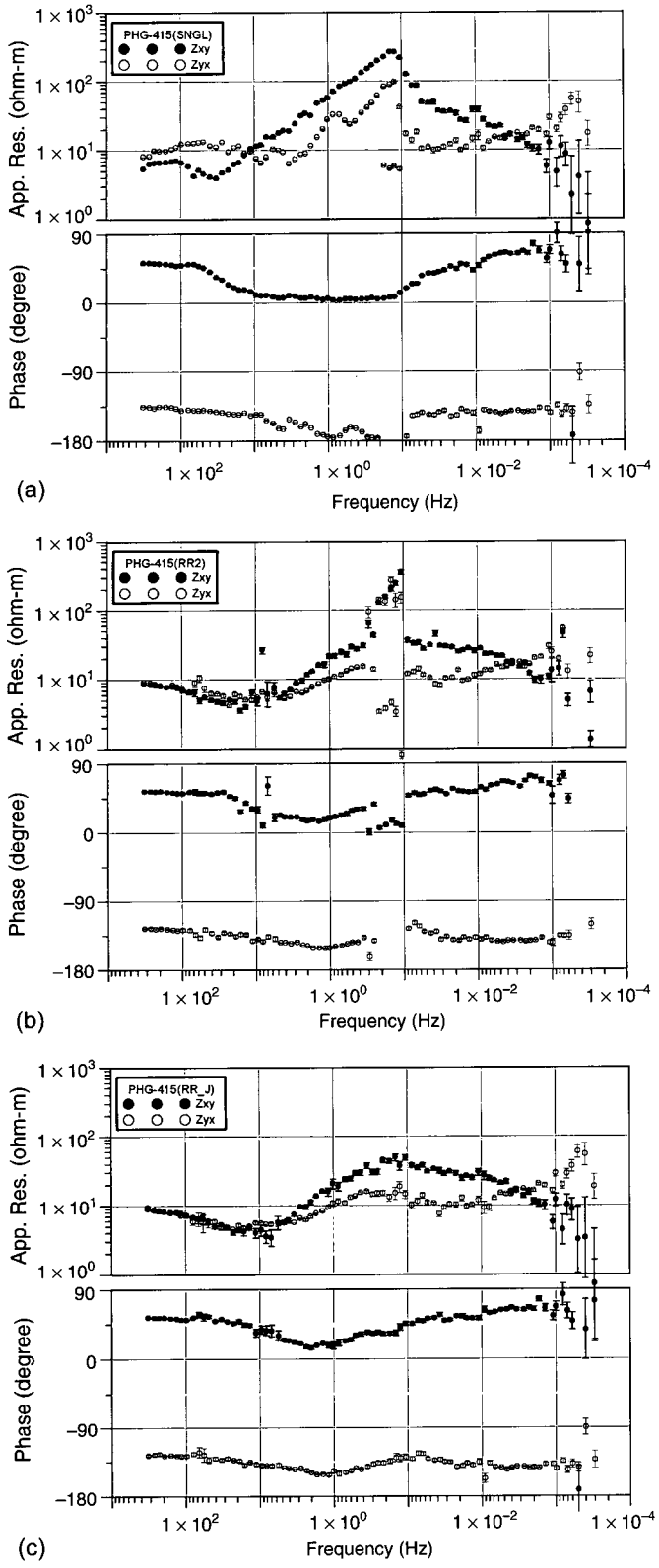

Fig. 3. Apparent resistivity and phase curves for the site PHG-415 calculated by (a) single site processing, (b) remote reference processing with RR2, and (c) with RR_J.

they point toward a low-resistivity zone (Rikitake and Honkura, 1985). The length of the arrow indicates the magnitude of induction vector; a long induction vector indicates that the horizontal variation of resistivity structure is severe and vice versa.

At 8 Hz, the vectors lengths are small and their directions are not systematic among stations. This means that the shallow parts of the section have minor resistivity variation in the horizontal direction and the section is nearly one-dimensional. A rough average apparent resistivity at 8 Hz is 10 Ω m, which corresponds to a skin depth of ~500 m. The induction vectors at 0.3 Hz point toward the south. Considering the fact that skin depth at this frequency reaches ~3–4 km, it is quite possible that a large low-resistivity body exists to the south of the survey area, at a distance or depth of 3–4 km. On the other hand, all the induction arrows at 0.01 Hz points toward the East Sea, in the south-east direction. As can be seen from Figure 2, the seashore lies 3~8 km from the survey area and is aligned in the north–south direction. Observed MT data will surely be affected by the nearby sea water.

3D MT modelling of the sea effect

To investigate the sea effect which may be contained in the observed MT data, a 3D model was set up, which included simplified coast lines and a layered structure inferred from the drilling results as shown in Figure 5. The resistivities of the layers down to 1.5 km was based on the drilling and logging results. Average depth to the sea floor and the resistivity of the sea water were assumed to be 1.5 km and 0.3 Ω m, respectively. Several simplifications were made in the model, namely: (a) the ocean bottom was considered flat, at 1.5 km depth, and (b) the ocean–continent transition is taken to be a sharp boundary following the simplified coastline, but neglecting the topography of the oceanic platform. 3D modelling for this model was performed using the staggered-grid finite difference code of Mackie et al. (1993). The total number of nodes was 70 (x) by 55 (y) by 23 (z, including 10 air layers).

Figure 6 shows the induction arrows calculated for frequencies 0.001, 0.005, 0.05, and 1 Hz, respectively. On the three panels in which frequencies are lower than 0.05 Hz, all of the induction arrows within the MT survey area point in the eastward direction, towards the sea. At 1 Hz on Figure 6d, however, the amplitude is very small, and the sea does not affect the MT response. Note that some arrows on the south-east margin of the survey region point to Youngil Bay, the nearest sea at that point, which means that the sea can affect the MT responses even up to 1 Hz, at the south-east margin of the survey region.

Apparent resistivity and phase curves for sites A and B, shown in Figure 5, are compared in Figure 7. These two sites correspond to the west- and east-most measuring point in this MT survey. Because the seashore boundary is the only two-dimensional structure in the model, the differences in apparent resistivities between xy- and yx-mode can only be a response to the sea effect. The split in apparent resistivity between the two modes appears at frequencies roughly below 0.2 Hz at site A, and below 1 Hz at site B. Thus, the nearby sea can affect the MT responses below the frequencies 0.2 Hz−1 Hz, depending on the station location. This result indicates that we need to consider the nearby sea in the interpretation of MT data below 1 Hz, although we have assumed a simplified coastline and a very sharp ocean–continent transition boundary.

3D MT inversion including sea floor

Of the 70 MT measurements, 44 measurements within the rectangle in Figure 2 were used for the 3D inversion. A linearised least-squares inversion with optimum regularisation and static shift parameterisation (Sasaki, 2004) was used for the inversion, in which forward modelling was done by the finite-

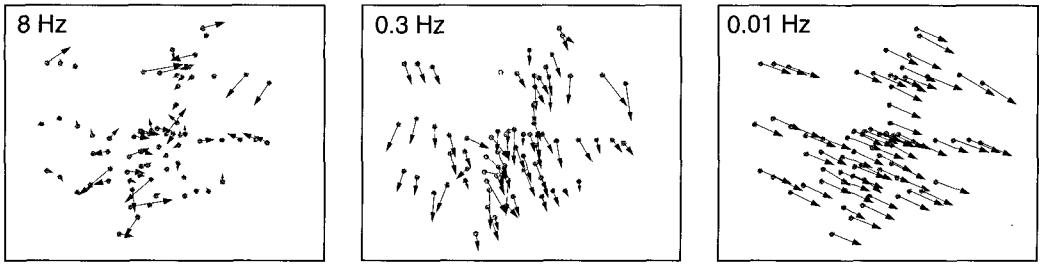

Fig. 4. Induction vectors at frequencies 8 Hz, 0.3 Hz, and 0.01 Hz, respectively. North is upward and extremely noisy data were omitted. Note that most of the arrows point to the sea in the east at 0.01 Hz, while they point to the south part at 0.3 Hz.

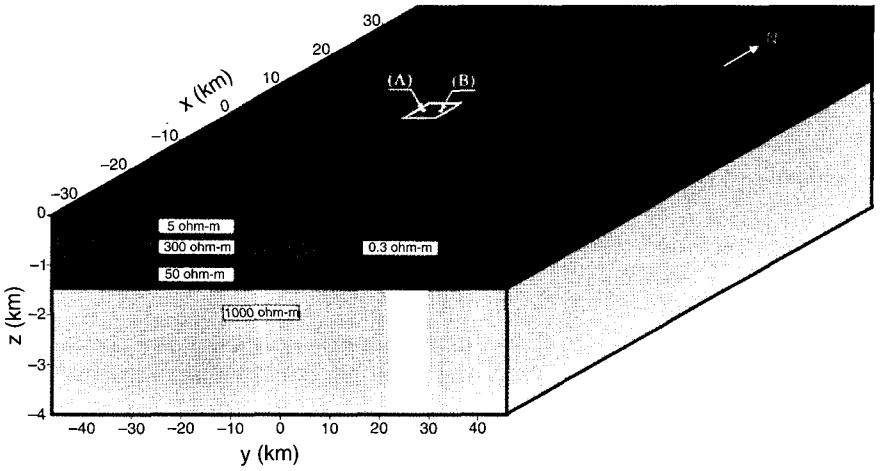

Fig. 5. A 3D model to investigate the sea effect in MT responses. The white box indicates the region under study. Note the arbitrary vertical scale.

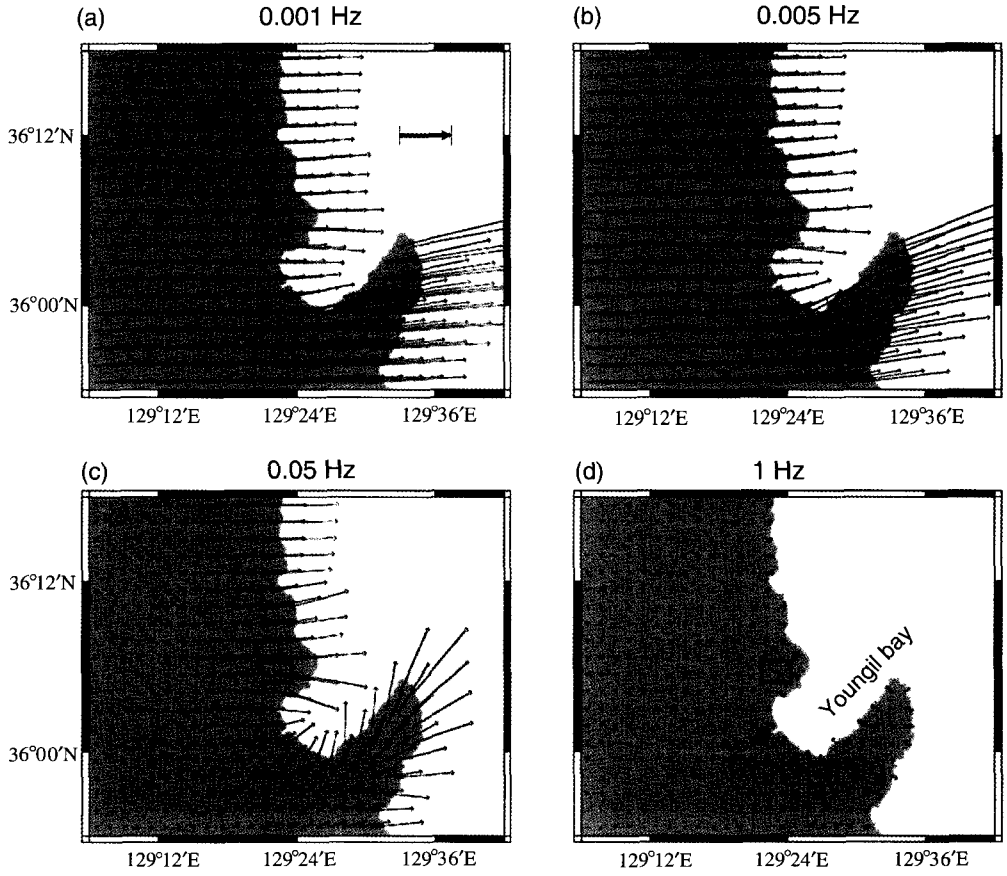

Fig. 6. In-phase induction vectors around Pohang geothermal sites at frequencies 0.001, 0.005, 0.05, 1 Hz, respectively, by 3D MT modelling with parameters shown in Figure 5. The box indicates the site under study and the length of the bold arrow at top-left in the figure indicates unit amplitude.

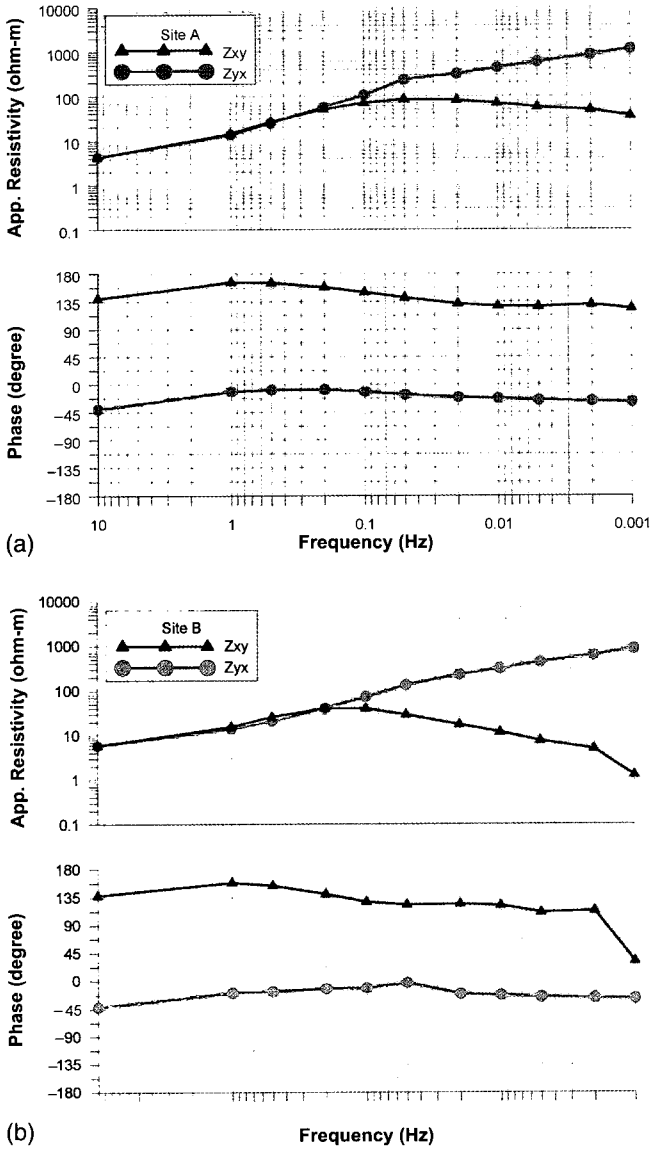

Fig. 7. Apparent resistivity and phase curves from the 3D MT modelling at site A and B shown in Figure 5. Note that the sea effect causes the split in apparent resistivities at low frequencies between *xy* and *yx* modes.

difference method. Some modifications were added to the code to implement seawater constraints. Weighting, for calculation of the data misfit, was based on the measurement error. A 3% noise floor was assumed. Thirteen frequencies were used, ranging from 0.0159 to 66 Hz. From 2288 apparent resistivity and phase data in *xy*- and *yx*-modes, 178 data with large measurement errors were excluded, so that 2110 data were used for the inversion. Cell size for forward modelling was 150 m in horizontal and 100 m in vertical directions at the surface of the target area, increasing in size outward and downward. The inversion model was divided into 2100 blocks, 10 × 15 × 14 blocks in *x*, *y*, and *z* directions, respectively. Including 88 static shift parameters in *xy*- and *yx*-modes at 44 sites, the total number of unknowns was 2188. The coordinate system used set the origin at the north-west-most measurement point, *x* to the east, *y* to the south, and *z* downward. The initial model was a homogenous half-space with resistivity of 14.65 Ω m, which was an average of observed apparent resistivities for all the input data. To include the sea water in the model, we assumed that the seashore boundary formed a straight line in the north–south direction (*y* direction) at $x = 9$ km, and that the sea continues infinitely to the east. The sea floor was assumed to be flat and located at a depth of 1.5 km. The input data and all other parameters are exactly the same in both inversions, except that we added some blocks to the eastern side of the model ($x \geq 9$ km) with fixed resistivity values during the inversion with sea water included. Resistivities of the sea water and the formation below the sea were fixed at 0.3 Ω m and 1000 Ω m, respectively, during the inversion process.

Figure 8 compares the inversion results with and without consideration of the nearby sea. The root-mean-square (RMS) errors at the final iteration were 2.78 for ordinary inversion (Figure 8a and 8c), and 2.19 for 3D inversion with seawater constraint (Figure 8b and 8d). Comparing these results, it can be easily seen that the shallow structure in both inversion results are very similar. The semi-consolidated sediment layer, with resistivity less than 10 Ω m, extends to 300–600 m in depth, as is already verified by test drilling. This layer appears to be thicker in the south and gets thinner to the north, as can be seen in Figure 8c and 8d. Beneath the sediment layer, there follows a layer 400–600 m thick with resistivity from several tens to a few hundreds of Ω m. Below this layer is a layer with resistivity of more than 300 Ω m.

The similarity between the two results comes from the fact that the sea affects only the low-frequency data, below 1 Hz, as discussed in 3D MT modelling section. If we assume the average resistivity of the formation to be ~10 Ω m, the skin depth at 1 Hz is ~1.6 km. Thus, in theory, the two results will show similar structures down to this depth at least.

At greater depths, however, the two results show quite different characteristics. Note in Figure 8a and 8c that a conductive (10–20 Ω m) layer appears at 3 km depth, and extends to the south-east. We also find a conductive layer at the same depth in Figure 8b and 8d. But this time the north-west direction is more conductive, and the eastern part shows rather resistive characteristics. 3D modelling results with the seashore included showed that MT data from the south-eastern part of the survey area would be strongly affected by Youngil Bay. If we omit the sea effect in the inversion, the sea effect present in the observed data will be projected onto the deeper part of the image. In that sense, the low-resistivity anomaly at 3 km depth in Figure 8a and 8c, at least the south-east part of it, seems to arise from the sea effect. In both cases, however, there seems to be a conductive structure at ~3 km depth. Further geological and geophysical study should follow to identify this structure.

Note that the inversion results including a seawater constraint show a conductive boundary below 1 km depth near the location of BH-2. The boundary extends in the north–south direction in Figure 8b, and also in the east–west direction in Figure 8d. The boundary can be related to two possible fractures intersecting at the location of the borehole, which is already expected from the lineament analysis from a satellite image, shown in Figure 1b.

Comparison with the drilling results

Based on the regional geological survey, lineament analysis from a satellite image, and a 2D interpretation of MT data obtained in 2002, two test boreholes (BH-1 and BH-2) were drilled in 2004, 165 m apart, at the location shown in Figure 2. BH-1 was designed for coring rock samples down to 1.1 km, and BH-2 reaches down to 1.5 km and was intended to characterise the geothermal aquifer by pumping tests.

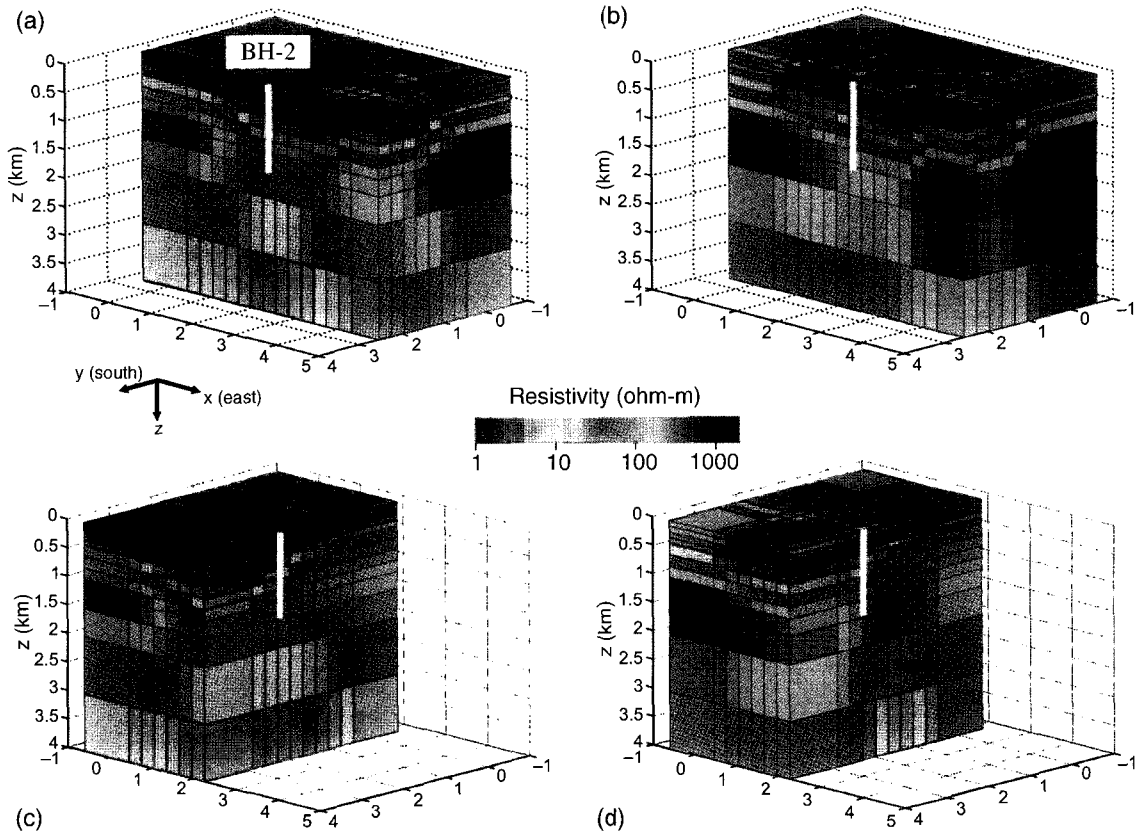

Fig. 8. Resistivity models from 3D inversions without any consideration of nearby sea (a and c), and with the sea as an inversion constraint (b and d). The location of test borehole (BH-2) is overlain on the figure. For (b) and (d), the seashore boundary is located at $x = 9$ km and extends in the north–south (y) direction. Depth to the sea floor is assumed to be 1.5 km. Conductivity of the sea water and the formation below is fixed to 0.3 Ω m and 1000 Ω m, respectively, during the inversion process.

Figure 9 shows the layered structures beneath the boreholes BH-1 and BH-2 based on logging of the cores and cuttings that comes from the drilling, and also shows a comparison between resistivity profiles from the resistivity log at BH-2 and those extracted from the 3D inversions.

Roughly four layers are revealed by the core logs: (a) a semi-consolidated mudstone (S-MS) extends from the surface down to the depth of ~360 m; (b) alternating appearance of trachybasalt (TB) and lapilli tuff (LT) within a mudstone layer; (c) intrusive rhyolite (RL) ~400 m thick; and (d) alternation of sandstone and mudstone (SS&MS) down to 1.5 km depth. The resistivity log shows that S-MS is very conductive, with resistivity below 10 Ω m; the region with TB and LT has resistivity of several tens of Ω m; RL shows resistivity of several hundreds of Ω m; and SS&MS has a resistivity of ~100 Ω m.

Both 3D inversions reconstruct the resistivity structure quite well, except for the resistive layer RL. As explained above, the results of the two inversions shows very similar characteristics down to a depth of 2 km, because the MT data are not affected by the sea at frequencies above 1 Hz.

There can be two possible reasons why the inversion did not resolve the layer RL. One is the physical limitation of the EM method — it is hard to resolve a thin resistive layer between conductive layers in nature. The other is the possibility of fracture systems running through the regions near the boreholes. We prefer the latter interpretation, because the inversion did resolve the RL layer, with resistivity of more than several hundred Ω m, in regions distant from the boreholes, as can be seen from Figure 8. Only the zone where BH-2 is located shows low resistivity and seems to have fractures extending to deeper formations. It is reported that the rocks and cores were severely fractured throughout the depth of the boreholes.

In addition, we used relatively large blocks in the inversion, so that the 3D inversion represents the average bulk resistivity of the inversion blocks, and the effect of fracture systems near the boreholes is reflected in the inversion results.

Conclusions

A three-dimensional (3D) magnetotelluric (MT) survey has been carried out to delineate subsurface structures and possible fractures, for development of low-temperature geothermal resources in Pohang, Korea. We could obtain quite good quality MT data throughout the survey region by locating the remote reference in Kyushu, Japan. The site is located in the south-eastern part of Korean peninsula and is very close to the eastern seashore. The survey area lies 3–8 km away from the seashore, which is aligned in the north–south direction. MT data are definitely affected by the nearby sea water, because of its extremely high conductivity compared to that of formation beneath the survey sites.

To infer the sea effect in the observed MT data, 3D MT modelling was performed for a layered model which included the sea water. Layering of the model and conductivities of each layer are roughly estimated from well logs and other geological information. Results showed that the conductive sea water affects the low frequency MT data, especially below 0.2–1 Hz, depending on the distance from the seashore. The most severe sea effect was observed from the south-east parts of the survey area because of the nearby seawater boundary at Youngil Bay.

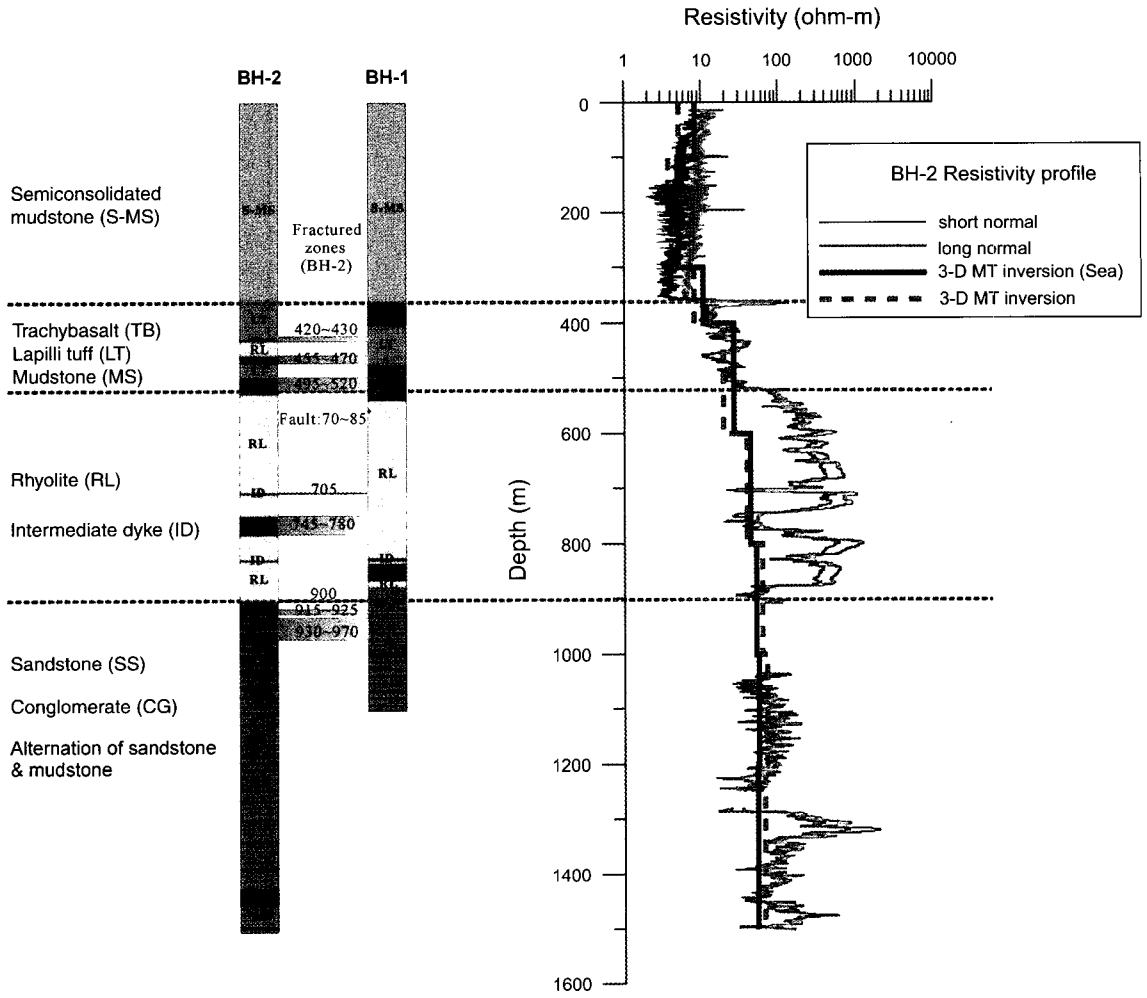

Fig. 9. A sketch of the layer structure including the two test boreholes (modified from Song, 2004) and a comparison between the resistivity profiles at the location of BH-2 from the resistivity log and from the resistivity model derived by 3D inversion.

Two kinds of 3D inversion have been performed with the MT data observed from the area; ordinary 3D inversion, and inversion including the sea as a constraint. The two resulting models showed very similar characteristics in their shallow parts, down to roughly 2 km. Comparison between the drilling results and the resistivity profiles from the inversions showed that the site can be described by a four-layered structure: from the top, (a) a semi-consolidated mudstone with resistivity less than 10 Ω m, with thickness of ~300 m in the northern part and ~600 m in the southern part of the survey area; (b) alternating appearance of trachybasalt and lapilli tuff within a mudstone layer with resistivity of a few tens of Ω m; (c) intrusive rhyolite, ~400 m thick, with resistivity of several hundreds of Ω m; and (d) alternating sandstone and mudstone down to 1.5 km depth, showing a resistivity of ~100 Ω m.

At greater depths, however, they showed very different characteristics, as can be expected from the modelling study. The strong effect of the nearby sea seems to form a fictitious conductive structure in the south-east part of the survey region, in ordinary 3D inversion. A conductive structure, however, was found at ~3 km depth from both inversions. More geological and geophysical study will be needed to identify this structure. Also, our study uses very simplified coastlines and sea floor bathymetry. Further studies should follow which include detailed seashore and seafloor descriptions as constraints, as well as specifying the resistivity of each layer beneath the sea bottom.

Acknowledgments

This work was supported by a Basic Research Project of the Korea Institute of Geoscience and Mineral Resources (KIGAM), funded by the Ministry of Science and Technology of Korea, and was conducted under a joint research program between KIGAM and the Geological Survey of Japan (AIST), Japan. We thank Dr Seong Kon Lee, Seong-Keun Lim, and In-Hwa Park for their help in the field, Dr Suk-Hoon Oh for performing the 3D modelling, and Dr Yutaka Sasaki for providing the 3D MT inversion code.

References

Bapat, V. J., Segawa, J., Honkura, Y., and Tarits, P., 1993, Numerical estimations of the sea effect on the distribution of induction arrows in the Japanese island arc: *Physics of the Earth and Planetary Interiors* **81**, 215–229. doi: 10.1016/0031-9201(93)90132-S

Mackie, R. L., Madden, T. R., and Wannamaker, P. E., 1993, Three-dimensional magnetotelluric modeling using difference equations – Theory and comparisons to integral equation solutions: *Geophysics* **58**, 215–226. doi: 10.1190/1.1443407

Monteiro Santos, F. A., Nolasco, M., Almeida, E., Pous, J., Marcuello, A., and Queralt, P., 1999, Correction of the ocean and coast effects on the magnetotelluric impedance tensor: *Second International Symposium on 3-D EM (3DEM-2)*, 309–312.

Monteiro Santos, F. A., Trota, A., Soares, A., Luzio, R., Lourenco, N., Matos, L., Almeida, E., Gaspar, J., and Miranda, J. M., 2006, An audio-magnetotelluric investigation in Terceria Island (Azores): *Journal of Applied Geophysics* **59**, 314–323. doi: 10.1016/j.jappgeo.2005.12.001

Oh, S., Yang, J., Lee, D. K., Kim, S.-K., Mogi, T., Nakada, M., and Song, Y., 2003, Study on deep structure of the Korean peninsula by GDS and teleseismic data: *Proceedings, 2003 Korea-Japan Joint Seminar on Geophysical Techniques for Geothermal Exploration and Subsurface Imaging*, 68–76.

Rikitake, T., and Honkura, Y., 1985, *Solid Earth Geomagnetism*, Terra Scientific Publishing.

Sasaki, Y., 2004, Three-dimensional inversion of static-shifted magnetotelluric data: *Earth. Planets and Space* **56**, 239–248.

Song, Y., 2004, Recent activities on low-temperature geothermal development in Korea: *Proceedings of the 6th Asian Geothermal Symposium*, 13–19.

Manuscript received 5 September 2006; accepted 15 December 2006.

포항지역 지열 개발을 위한 3 차원 자기지전류 탐사

이태종[1], 송윤호[1], Toshihiro Uchida[2]

요 약: 포항 저온 지열개발 지역에서 지하구조 규명 및 파쇄대 탐지를 목적으로 3 차원 자기지전류 (MT)탐사를 실시하였다. 현장에서 약 480 km 떨어진 일본 큐슈 지역에 원거리 기준점을 설치하여 양질의 자료를 획득하였다.

대상지역이 바다에 인접한 관계로 바다의 효과를 고려한 3 차원 모델링과 역산을 수행하여 측정된 MT 탐사자료에 포함된 바다효과를 고찰하였다. 그 결과 포항지역에 인접한 바다는 해안선으로부터의 거리에 따라 1 Hz ~ 0.2 Hz 이하의 주파수대에 주로 영향을 미치며, 특히 영일만에 인접한 남동쪽의 측점들이 바다의 영향을 가장 크게 받은 것으로 나타났다.

약 2 km 심도 이하의 천부에서는 인접한 바다를 3 차원 역산에 포함시킨 경우와 그렇지 않은 경우가 매우 비슷한 결과를 보였으나, 이보다 심부의 경우는 바다를 포함시키지 않은 3 차원 역산에서 대상지역의 남동쪽에 저비저항 구조가 나타나는데 이는 인접 바다의 영향이 투영되어 나타난 것으로 보인다.

시추 결과 및 역산에 의한 전기비저항 구조를 비교한 결과 대상지역의 지하를 크게 다섯 개의 층으로 구분할 수 있었다. 즉: 1) 10 ohm-m 이하의 전기비저항을 보이는 반고결이암층이 대상지역 북쪽에서는 지표로부터 약 300 m, 남쪽에서는 약 600 m 의 두께로 분포하고; 2) 이암층 내에 수십 ohm-m 의 전기비저항을 보이는 화산력응회암 및 조면현무암이 교대로 나타나며; 3) 수백 ohm-m 의 전기비저항을 갖는 유문암이 약 400 m 의 두께로; 4) 이후 약 1.5 km 까지는 약 100 ohm-m 의 전기비저항을 보이는 사암 및 이암층이 분포하며; 5) 약 3 km 심도에서 저비저항 구조가 나타나는데 이 층에 대해서는 추가적인 지질학적, 지구물리학적인 조사가 필요할 것으로 생각된다.

주요어 : 3 차원 MT 탐사, 원거리기준점 MT, 바다효과, 지열탐사

韓国ポハン地域における地熱開発のための３次元 MT 法探査

李 泰鍾（イ・テジョン）[1], 宋 允鎬（ソン・ユンホ）[1], 内田 利弘[2]

要 旨: 韓国ポハン（浦項）地域における低温地熱資源の開発のため，同地域の地質構造と破砕帯分布の解明を目的として３次元 MT 法探査を実施した。調査地から約 480 km 離れた九州南部（日本）にリモートリファレンス点を置いて参照処理を行うことにより，調査地周辺の強い電磁ノイズを除去し，良質な測定データを得ることができた。

調査地が東海（日本海）に近接しているため，海水の影響を考慮した３次元モデリングとインバージョンを行い，MT 法データに含まれる海洋効果について考察した。その結果，海水の影響が現れる周波数は海岸線からの距離に依存するが，調査地では 1 Hz ~ 0.2 Hz 以下の周波数帯で影響を受けており，特に，ヨンイル（迎日）湾に近い南東部の測点で海水の影響が強いことがわかった。海洋効果を考慮した３次元インバージョンと考慮しないインバージョンを行って得られたモデルを比較したところ，約 2km より浅い部分の比抵抗構造は両者でほとんど同じ結果が得られたが，2km より深い部分については海洋効果を考慮しない３次元インバージョンでは当該地域の南東部に低比抵抗構造が見られた。これは海洋効果によるものであると考えられる。

３次元インバージョンによって得られた比抵抗構造を地熱開発のために掘削された坑井のデータと比較した結果，当該地域を特徴づける地層として以下の５層が推定された。すなわち，1) 調査域北部では地表から約 300m まで，南部では約 600m の深さまで，10 Ωm 以下の低比抵抗の半固結泥岩層が分布する。 2) その下位には数十Ωm の比抵抗を有する泥岩中に火山礫凝灰岩と粗面玄武岩の層が交互に存在する。3) その下位には数百Ωm の比抵抗を有する流紋岩が約 400m の厚さで分布する。4) その下には深度約 1.5km まで約 100 Ωm の比抵抗の砂岩と泥岩層が分布している。そして，5) 深さ約 3km に低比抵抗層が解析されたが，これについては追加的な地質学的，地球物理学的調査が必要であると考えられる。

キーワード：３次元 MT 法探査，リモートリファレンス MT，海洋効果，地熱探査

1 한국지질자원연구원 지하수지열연구부
305-350 대전시 유성구 가정동 30
2 산업기술종합연구소 지권자원환경연구부문

1 韓国地質資源研究院 地下水地熱研究部
2 産業技術総合研究所 地圏資源環境研究部門